JOURNAL OF VIROLOGY, Sept. 1981, p. 823-834
0022-538X/81/090823-12$02.00/0

Vol. 39, No. 3

Mouse Hepatitis Virus A59: mRNA Structure and Genetic Localization of the Sequence Divergence from Hepatotropic Strain MHV-3

MICHAEL M. C. LAI,* PETER R. BRAYTON, ROBERT C. ARMEN, CHRIS D. PATTON, CHARLES PUGH,† AND STEPHEN A. STOHLMAN

Departments of Microbiology and Neurology, University of Southern California School of Medicine, Los Angeles, California 90033

Received 9 April 1981/Accepted 26 May 1981

The composition and structure of the mouse hepatitis virus (MHV)-specific RNA in actinomycin D-treated, infected L-2 cells were studied. Seven virus-specific RNA species with molecular weights of 0.6×10^6, 0.9×10^6, 1.2×10^6, 1.5×10^6, 3.0×10^6, 4.0×10^6, and 5.4×10^6 (equivalent to the viral genome) were detected. T_1 oligonucleotide fingerprinting studies suggested that the sequences of each RNA species were totally included within the next larger RNA species. The oligonucleotides of each RNA species were mapped on the 60S RNA genome of the virus. Each RNA species contained the oligonucleotides starting from the 3′ end of the genome and extending continuously for various lengths in the 3′ → 5′ direction. All of the viral RNA species contained a polyadenylate stretch of 100 to 130 nucleotides and probably identical sequences immediately next to the polyadenylate. These data suggested that the virus-specific RNAs are mRNA's and have a stairlike structure similar to that of infectious bronchitis virus, an avian coronavirus. A proposal is presented, based on the mRNA structure, for the designation of the genes on the MHV genome. Using this proposal, the sequence differences between A59, a weakly pathogenic strain, and MHV-3, a strongly hepatotropic strain, were localized primarily in mRNA's 1 and 3, corresponding to genes *A* and *C*.

Murine hepatitis viruses (MHVs) are members of the Coronaviridae, which include viruses isolated from many species of animals (10, 18). They contain a positive single-stranded 60S RNA genome with a molecular weight of 5.4×10^6 (6, 7, 19). Several other coronaviruses have been reported to have a similar genome structure (4, 8, 9). A viral genome of this size can code for all of the MHV structural proteins, which include gp180/90, pp50, and gp23 (17), and may also have enough information to code for several nonstructural proteins (6). However, no attempts have yet been made to localize the genetic regions which code for the possible gene products.

Our laboratories have been interested in identifying the genetic regions of the MHV genome associated with various viral properties, particularly those responsible for the ability of the virus to cause different diseases. Recently, we have shown that the genomic RNAs of a weakly pathogenic strain, A59, and a strongly hepatitis-inducing strain, MHV-3, have very similar oligonucleotide fingerprints except for a few oligonucleotides (7). We have also found that a demyelination-inducing MHV strain, JHM-DS, and a JHM strain which causes very little demyelination, JHM-DL, differ in only a few oligonucleotides (S. A. Stohlman, M. M. C. Lai, and L. Weiner, unpublished data). These viruses thus provide a potential system for the identification of genetic regions responsible for viral pathogenicity. As an initial step toward this purpose, we studied the structure of the intracellular viral RNAs in order to identify the mRNA species which are transcribed from such genetic regions.

Several earlier reports have attempted to characterize the virus-specific mRNA in MHV-infected cells (11, 12). In these studies, only a few RNA species of 18 to 28S were detected. These RNAs are not likely to represent the total RNA species transcribed from the MHV genome. Recently, Stern and Kennedy (14, 15) found six mRNA species in the avian coronavirus-infected cells. Furthermore, they showed that these mRNA's had a nested strucutre. Several laboratories have also found seven mRNA species in MHV-infected cells (13; J. Leibowitz, personal communication). In this report, we

show that the mRNA's of similar nature exist in MHV-A59-infected cells. We have further characterized their structure.

MATERIALS AND METHODS

Viruses and cells. The A59 strain of MHV was originally obtained from C. Bond, of the University of California at San Diego. This strain has been shown to be weakly pathogenic (11). The hepatotropic MHV-3 strain was obtained from M. Collins, of Microbiological Associates, Bethesda, Md. The L-2 cells were obtained from L. Sturman, New York State Department of Health, Albany, N.Y. The DBT cell line was obtained from K. Fujiwara, University of Tokyo, Japan. Viruses were plaque purified on DBT cells before use.

Radiolabeling and purification of virus. For preparation of ^{32}P-labeled viral RNA, the viruses were grown on monolayers of DBT cells in 15-cm dishes. Virus was adsorbed at a multiplicity of infection of one to five at 37°C for 1 h. After adsorption, the inoculum was removed, and 25 ml of Dulbecco modified minimum essential media (DMEM) containing 1% heat-inactivated (56°C for 30 min) fetal calf serum (FCS) was added. After 4 h at 37°C, the medium was removed and replaced with phosphate-free DMEM which contained 1% dialyzed FCS and 200 μCi of $^{32}P_i$ per ml (ICN Pharmaceuticals). Supernatant fluids were collected 8 h later and cleared of cell debris by centrifugation at 15,000 × *g* for 30 min at 4°C. Virus was then pelleted and purified by sedimentation on linear 20 to 42% sucrose gradients as previously described (6). The ^{32}P-labeled RNA was extracted from the purified virus according to published procedures (7).

Preparation of intracellular virus-specific RNA. DBT and L-2 cells were used to prepare intracellular virus-specific RNA. Both cell lines were infected with MHV-A59 at a multiplicity of one to five for 1 h at 37°C. After adsorption, DMEM which contained 2% dialyzed FCS and 1 to 3 μg of actinomycin D per ml (a gift of Merck Sharp & Dohme) was added. At 3 to 4 h postinfection, 100 μCi of [^{3}H]uridine per ml was added, and the virus-specific RNA was extracted at 6 to 7 h postinfection. L-2 cells were used to prepare ^{32}P-labeled RNA because the RNA synthesis in DBT cells was markedly reduced when the cells were incubated in phosphate-depleted medium. L-2 cells were incubated for 6 to 8 h in DMEM containing 2% dialyzed FCS and 1/10 of the normal concentration of phosphate before infection. After infection, the L-2 cells were cultured in phosphate-free DMEM which contained 2% dialyzed FCS, 3 μg of actinomycin D per ml, and 250 μCi of $^{32}P_i$ per ml. Virus-specific RNA was extracted from L-2 cells at 7 to 9 h postinfection.

For extraction of intracellular viral RNA, monolayers of infected cells were chilled on ice and washed three times with SS buffer (10 mM Tris, 60 mM NaCl, and 1 mM EDTA, pH 8.5). The cells were lysed in the SS buffer containing 0.5% Triton N-101, and the nuclei were removed by centrifugation at 1,800 × *g* for 5 min. The supernatant fluid was then adjusted to contain 1% sodium dodecyl sulfate (SDS) and was extracted at 4°C with chloroform-phenol (1:1). The RNA was precipitated by the addition of 2 volumes of ethanol at −20°C overnight.

Initially, the RNA was analyzed by velocity sedimentation in linear 15 to 30% sucrose gradients prepared in SS buffer (pH 8.0) which contained 0.5% SDS. Centrifugation was performed in an SW40 rotor at 20,000 rpm for 16 to 20 h at 20°C. Fractions (0.2 ml) were collected with an ISCO fraction collector and were monitored by UV absorbance at 254 nm. ^{32}P-labeled DBT cellular RNA was added to provide 28S, 18S, and 4S sedimentation markers.

Agarose gel electrophoresis. Two different conditions were used for agarose gel electrophoresis. In most of the experiments, the RNA samples were dissolved in RE buffer (50 mM boric acid, 5 mM sodium borate, 1 mM EDTA, and 10 mM sodium sulfate, pH 8.1), heat denatured by boiling at 100°C for 1 min, and electrophoresed in 1% agarose gel slabs (15 by 20 by 0.3 cm) made in RE buffer at 90 V for 5 h. For determination of molecular weights of RNAs, the RNA samples were dissolved in RE buffer and electrophoresed in agarose gel slabs made in RE buffer containing 5 mM methylmercuric hydroxide (2). After electrophoresis, the gels were wrapped with cellophane and exposed to Kodak XR film with an intensifying screen for various periods of time.

For preparative gel electrophoresis, the RNA samples were electrophoresed in agarose gels with or without methylmercuric hydroxide as described above. The RNA bands were excised from the gel, suspended in 2 to 3 ml of distilled water, and crushed with a Dounce homogenizer. For RNAs excised from the methylmercury gels, the gel slices were first washed with two changes of 0.5 M ammonium acetate before homogenization. After centrifugation at 20,000 × *g* for 15 min to remove the gel, the supernatant was adjusted to 0.15 M ammonium acetate and precipitated with 2.5 volumes of ethanol. This extraction procedure removed at least 80% of the radioactivity. Further elution of the gel did not remove additional RNA. The RNA was precipitated by sedimentation at 20,000 × *g* for 15 min and redissolved in 0.4 ml of 0.2 M ammonium acetate. The RNA samples were again centrifuged at 20,000 × *g* for 15 min to remove contaminating gel pieces. The RNA in the supernatant was finally precipitated with 2.5 volumes of ethanol.

Oligonucleotide fingerprinting. The ^{32}P-labeled RNA extracted from purified virions or eluted from gels was digested with RNase T_1 and analyzed by two-dimensional polyacrylamide gel electrophoresis essentially as previously described (7). Briefly, the first dimension was performed on 10% polyacrylamide–0.125% bisacrylamide gel slabs in citrate buffer, pH 3.3, containing 6 M urea. Electrophoresis was carried out at 700 V for 4 h. The second dimension was performed on 22% polyacrylamide gel–0.15% bisacrylamide gel slabs in Tris-borate buffer, pH 8.0, at 600 V for 16 h. After electrophoresis, the gels were wrapped with cellophane and exposed to Kodak BB-1 film with an intensifying screen at 4°C.

Oligonucleotide mapping. The ^{32}P-labeled 60S RNA was dissolved in 0.3 ml of 0.05 M sodium carbonate and incubated at 50°C for 1 to 5 min. The reaction mixture was then neutralized with 15 μl of 1 M acetic acid and precipitated with 2.5 volumes of ethanol. The RNA was pelleted by sedimentation at 20,000 × *g* for 15 min and was then fractionated by oligodeoxythymidylate [oligo(dT)]-cellulose column chromatography

according to the procedure of Aviv and Leder (1). In the later part of the experiments, the alkali digestion of the RNA was omitted. Instead, the total RNA from purified virus, without prior separation by sucrose gradient sedimentation, was used directly for oligo(dT)-cellulose chromatography. The RNA prepared by this procedure was degraded enough for oligonucleotide mapping. The polyadenylate [poly(A)]-containing RNA selected by oligo(dT)-cellulose chromatography was sedimented in a 10 to 25% sucrose gradient made in 0.01 M Tris-hydrochloride, pH 7.4, 0.01 M NaCl, and 0.05% SDS in an SW41 rotor at 40,000 rpm for 4.5 h. The RNAs of different sizes were pooled separately and were used for T_1 oligonucleotide fingerprinting.

Base sequence analysis. The poly(A)-containing oligonucleotides separated by two-dimensional polyacrylamide gel electrophoresis were excised from the gels, eluted with 0.5 ml of 0.5 M NaCl, and precipitated with 2.5 volumes of ethanol. The oligonucleotides were pelleted by sedimentation at 20,000 × *g* for 15 min, redissolved in 10 μl of water which contained RNase A at 0.1 mg/ml, and incubated at 37°C for 30 min. After incubation, the digests were spotted on DEAE-cellulose paper and electrophoresed in acetic acid-pyridine buffer (pH 3.5) at 1,500 V until the xylene-cyanol dye had traveled 15 cm. The DEAE-cellulose paper was dried and exposed to Kodak BB-1 film with intensifying screens. The base composition of the oligonucleotides was determined by comparison with nucleotide standards obtained by digestion of the total unfractionated RNA (see Fig. 7) (3). Each spot was cut out of the paper and was counted in toluene-based scintillation fluid. The relative ratio of each nucleotide was determined from the radioactivity present in each spot.

RESULTS

Kinetics of intracellular viral RNA synthesis. MHV infection of L-2 or DBT cells did not result in inhibition of host cell macromolecular synthesis (data not shown). Therefore, to study the intracellular viral RNA, the RNA synthesis of the host cells was inhibited by addition of actinomycin D. We found that, with actinomycin D at a concentration of 1 μg/ml for DBT cells and 3 μg/ml for L-2 cells, the host RNA synthesis was completely inhibited. At these concentrations, no appreciable effect of actinomycin D on viral replication was noticed, as judged by the kinetics of virus growth, virus yield, and cytopathic effects. Similar observations have also been made by Robb and Bond (11). However, at higher concentrations of actinomycin D (5 μg/ml), the yield of infectious virus from DBT cells was reduced by 100-fold. L-2 cells were more resistant to actinomycin D, and there was no appreciable reduction in virus yield even at 5 μg/ml. We therefore used actinomycin D at 1 μg/ml for DBT cells and at 3 μg/ml for L-2 cells throughout this study.

We first determined the kinetics of the intracellular virus-specific RNA synthesis in DBT cells. The cells were infected with MHV-A59 at a multiplicity of one to five and were labeled with [^{3}H]uridine for 1 h at various times after infection. Table 1 shows the rate of viral RNA synthesis and virus yields at different time points postinfection. After a lag of 2 h, the virus-specific RNA synthesis reached a peak at 6 to 7 h postinfection. Thereafter, the rate of viral RNA synthesis declined. By contrast, the titer of the infectious virus released into the medium did not reach its peak until 8 to 9 h postinfection. For most of the studies, we used intracellular viral RNA which was prepared during maximum intracellular RNA synthesis. Studies performed with L-2 cells cultured in the presence of 3 μg of actinomycin D per ml yielded similar data (Table 1), with the only exception being that maximum RNA synthesis was delayed by 1 h in L-2 cells compared with DBT cells.

Sucrose gradient sedimentation and electrophoretic analysis of MHV-specific RNA. To determine the species and structure of the virus-specific RNA in the MHV-infected cells, the A59-infected DBT or L-2 cells were labeled with [^{3}H]uridine or $^{32}P_i$, and the total cytoplas-

TABLE 1. *Rate of MHV-A59 virus-specific RNA synthesis in DBT and L-2 cells*

Cell[a]	Time post-infection (h)	Radioactivity[b] (cpm)	Virus yield (PFU/ml)[c]	
			−AMD	+AMD
DBT	2	0	1×10^2	8×10^1
	3	650	4×10^3	2×10^3
	4	2,700	2×10^4	3×10^4
	5	4,600	5×10^4	5×10^4
	6	23,000	4×10^5	4×10^5
	7	11,200	3×10^6	3×10^6
	8	2,850	4×10^6	1×10^6
	9	1,470	5×10^6	2×10^6
L-2	4	0	2×10^3	2×10^4
	6	680	3×10^3	2×10^4
	7	1,320	1×10^4	2×10^5
	8	3,620	2×10^5	4×10^6
	9	510	3×10^6	8×10^6
	10	480	2×10^6	3×10^5
	11	420	8×10^5	4×10^5

[a] DBT cells were treated with actinomycin D (AMD) at 1 μg/ml and [^{3}H]uridine at 100 μCi/ml. L-2 cells were treated with actinomycin D at 3 μg/ml and [^{3}H]uridine at 10 μCi/ml. The cells were labeled for 1 h at the specified time postinfection. After labeling, the cells were disrupted with 1% SDS, and the amount of [^{3}H]uridine incorporation was determined by precipitation with trichloroacetic acid.

[b] The amount of trichloroacetic acid-insoluble [^{3}H]uridine incorporation after labeling for 1 h in the A59-infected cells in the presence of actinomycin D. Counts of the uninfected cells have been subtracted.

[c] Determined by plaque assay on DBT cells.

mic RNA was subjected to sucrose gradient sedimentation. At least four RNA species could be detected: 60S, 32S, 22S, and 18S (Fig. 1). The 60S RNA cosedimented with the genomic RNA extracted from the purified virus (Fig. 1b). Furthermore, the T_1 oligonucleotide fingerprint of this RNA was identical to that of the 60S viral genomic RNA (see below). Therefore, this RNA species represented the genomic RNA of the virus. The rest of the RNAs represented the virus-specific subgenomic RNAs, since the mock-infected, actinomycin D-treated cells did not contain any RNA of this size (Fig. 1a). An additional species of RNA, 4S, likely represented the tRNA's which were found in the uninfected cells as well. This RNA species was not further characterized.

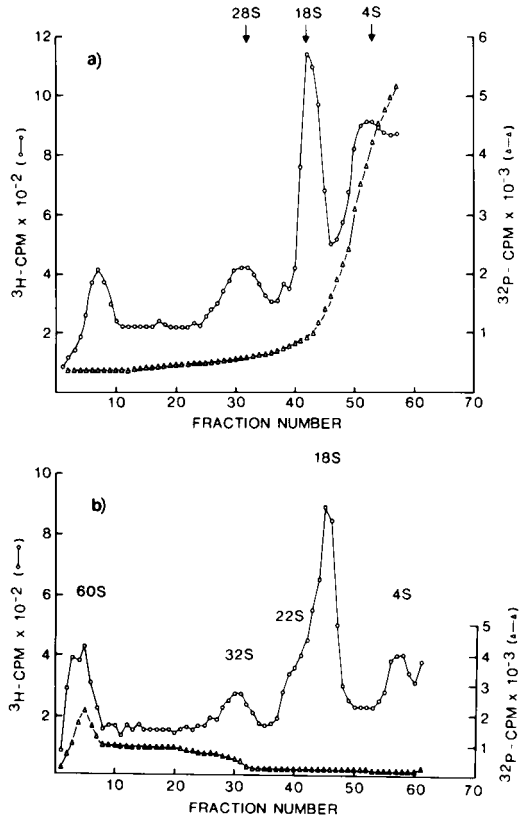

FIG. 1. *Sucrose gradient sedimentation of the virus-specific RNA in the MHV-infected cells. [^{3}H]uridine-labeled RNA was extracted from the MHV-A59-infected and actinomycin D-treated DBT cells at 7 h postinfection and then sedimented through a 15 to 30% linear sucrose gradient containing 0.5% SDS in an SW40 rotor at 20,000 rpm for 20 h. (a) The ^{32}P-labeled RNA from the mock-infected and actinomycin D-treated DBT cells was cosedimented. (b) The ^{32}P-labeled 60S RNA extracted from the purified MHV-A59 virion was included for comparison. The positions of the 28S, 18S, and 4S marker RNAs are indicated.*

The virus-specific RNAs were further separated by electrophoresis on 1% agarose gels. Six virus-specific RNA bands could be resolved (Fig. 2a). Longer exposure of the gels did not reveal any additional RNA bands. When these RNAs were analyzed by electrophoresis on denaturing gels which contained methylmercuric hydroxide (2), essentially similar results were obtained. Six RNA species were consistently resolved (Fig. 2b). However, in a few RNA preparations, an additional RNA species was found (Fig. 2c). These findings confirmed the data recently obtained in other laboratories with the A59-infected Sac (−) or 17 Cl-1 cells, which also contained seven virus-specific RNA species (13; H. Wege, S. Siddell, M. Sturm, and V. ter Meulen, *in* V. ter Meulen, S. Siddell, and H. Wege, ed., *Biochemistry and Biology of Coronaviruses*, in press; J. Leibowitz, personal communication). We designated these RNAs, in order of decreasing size, RNA species 1 through 7. The molecular weights of these RNA species were determined from the migration rates of the RNAs in the agarose gels containing methylmercuric hydroxide (Fig. 2b, c). Under these conditions, the migration rate of the RNA was inversely proportional to the logarithm of the molecular

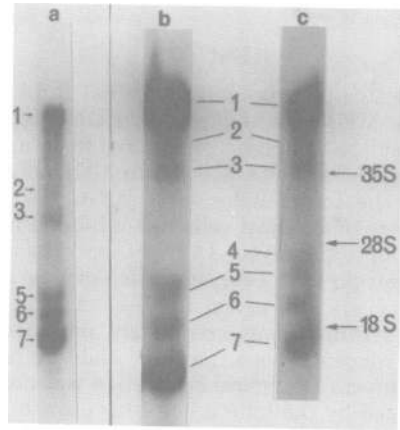

FIG. 2. *Agarose gel electrophoresis of the virus-specific RNA in the A59-infected cells. The ^{32}P-labeled RNA from the A59-infected L-2 cells was heat denatured at 100°C for 1 min and electrophoresed on 1% agarose gel without (a) or with (b and c) methylmercuric hydroxide at 90 V for 5 h. The RNAs in (a), (b), and (c) were from different preparations. The positions of the 35S Rous sarcoma virus RNA and 28S and 18S rRNA's are indicated. The gels in (b) and (c) were overexposed to reveal the lesser RNA species.*

weight (2). From these data, the molecular weights of the intracellular virus-specific RNAs were determined to be 5.4×10^6, 4.0×10^6, 3.0×10^6, 1.5×10^6, 1.2×10^6, 0.9×10^6, and 0.6×10^6 for RNA species 1 through 7, respectively.

It is noteworthy that the relative ratio of these RNA species remained quite constant, with the exception of RNAs 1 and 4. RNA 1 (equivalent to the viral genome) was the most variable species. In some preparations, it was the predominant RNA species (Fig. 2b, c). It is probable that the ratio of all the subgenomic RNA species remained constant, whereas the increase of RNA 1 was due to accumulation of genomic RNA destined to be incorporated into the virion. RNA 4 was present in the lowest amount in all of the RNA preparations. In L-2 cells, this RNA species was usually not detectable.

Oligonucleotide fingerprinting of the virus-specific RNAs. The sum of the molecular weights of the six subgenomic RNAs exceeded the genome size, suggesting that these RNAs overlap in their sequences. To determine the structural relationship between the various RNA species, oligonucleotide fingerprints of every virus-specific RNA, except RNA 4, which was usually not detectable in our system, were examined. The ^{32}P-labeled RNAs were eluted from agarose gels, digested with RNase T_1, and separated by two-dimensional polyacrylamide gel electrophoresis. The T_1 oligonucleotide fingerprints became increasingly complex as the size of the RNAs increased (Fig. 3). Furthermore, most of the oligonucleotides present in the small RNA species were included in the fingerprints of the next larger RNA species. Also, most of the oligonucleotides in each RNA species were also present in the 60S genomic RNA of MHV-A59, suggesting that they represented sequences of the same polarity as the genomic RNA. The RNA 1 had an oligonucleotide fingerprint identical to that of the genomic RNA, confirming that RNA 1 represents the intracellular form of the genomic RNA. Finally, every RNA species contained a poly(A) spot (located at the lower left corners of the fingerprints), indicating that they are polyadenylated and probably function as mRNA's.

The oligonucleotide fingerprints of several of the RNA species also contained some anomalous oligonucleotides: (i) RNA 7 contained an oligonucleotide, 19, which was present only very weakly or not at all in other subgenomic RNA species; (ii) RNA 6 contained an oligonucleotide, 19a, and RNA 5 contained an oligonucleotide, 3a, both of which were not present in the viral genome, nor were they detected in other subgenomic RNA species; (iii) RNAs 2 and 3 were slightly contaminated with the degradation products of RNA 1; however, the contaminating oligonucleotides could be discerned due to the much lower molar ratio at which they occurred (Fig. 3). It appeared that the amounts of some of the oligonucleotides, e.g., oligonucleotides 3 and 5 in RNA 3, were reduced in RNA 2. The origin of these anomalous oligonucleotides is currently being studied. It is possible that these oligonucleotides represent the extreme 5′ ends of the subgenomic RNA species.

Mapping of the subgenomic RNA species on the RNA genome. The oligonucleotide fingerprints of the virus-specific RNA species suggested that the MHV subgenomic RNAs had overlapping sequences, with the sequences of the smaller RNA being contained within the next-larger RNA species. However, these studies did not reveal the genetic localization of these mRNA's on the RNA genome. It was important to determine the genetic regions from which each mRNA species was transcribed. To accomplish this, we studied the map position of each oligonucleotide on the RNA genome. The partially degraded ^{32}P-labeled 60S RNA of A59 was fractionated by chromatography on oligo(dT)-cellulose. The poly(A)-containing RNA was selected and fractionated by sucrose gradient sedimentation. The genomic RNA from A59 was degraded to such an extent that the peak size of the RNA was 18S (Fig. 4). The poly(A)-containing RNAs of different sizes were pooled as shown in Fig. 4 and analyzed by T_1 oligonucleotide fingerprinting. Several of the RNA fingerprints are presented in Fig. 5. All these RNAs contained the sequences starting from the 3′ end and extending for various distance toward the 5′ end of the genome. Therefore, the relative position of each oligonucleotide on the RNA genome could be arranged in several groups from 3′ toward the 5′ end. Furthermore, the position of the oligonucleotides on the RNA genome could be estimated from the smallest size of the poly(A)-containing RNA in which the oligonucleotide was detected. By this approach, all the oligonucleotides of the genomic RNA of MHV-A59 were mapped in several groups on the genome (Fig. 6). By comparison with this oligonucleotide map, it was found that all of the oligonucleotides in RNA 7 were located at the 3′ end of the genome. The rest of the virus-specific RNAs also contained the oligonucleotides starting from the 3′ end and extending for various lengths toward the 5′ end (Fig. 6). This result suggested that the subgenomic RNAs of MHV-A59 had a structure similar to that proposed for avian infectious bronchitis virus (14, 15). However, it was also clear from Fig. 6 that several RNA species, including 2, 3, 5, and 6, contained the oligonucleotides which either were absent

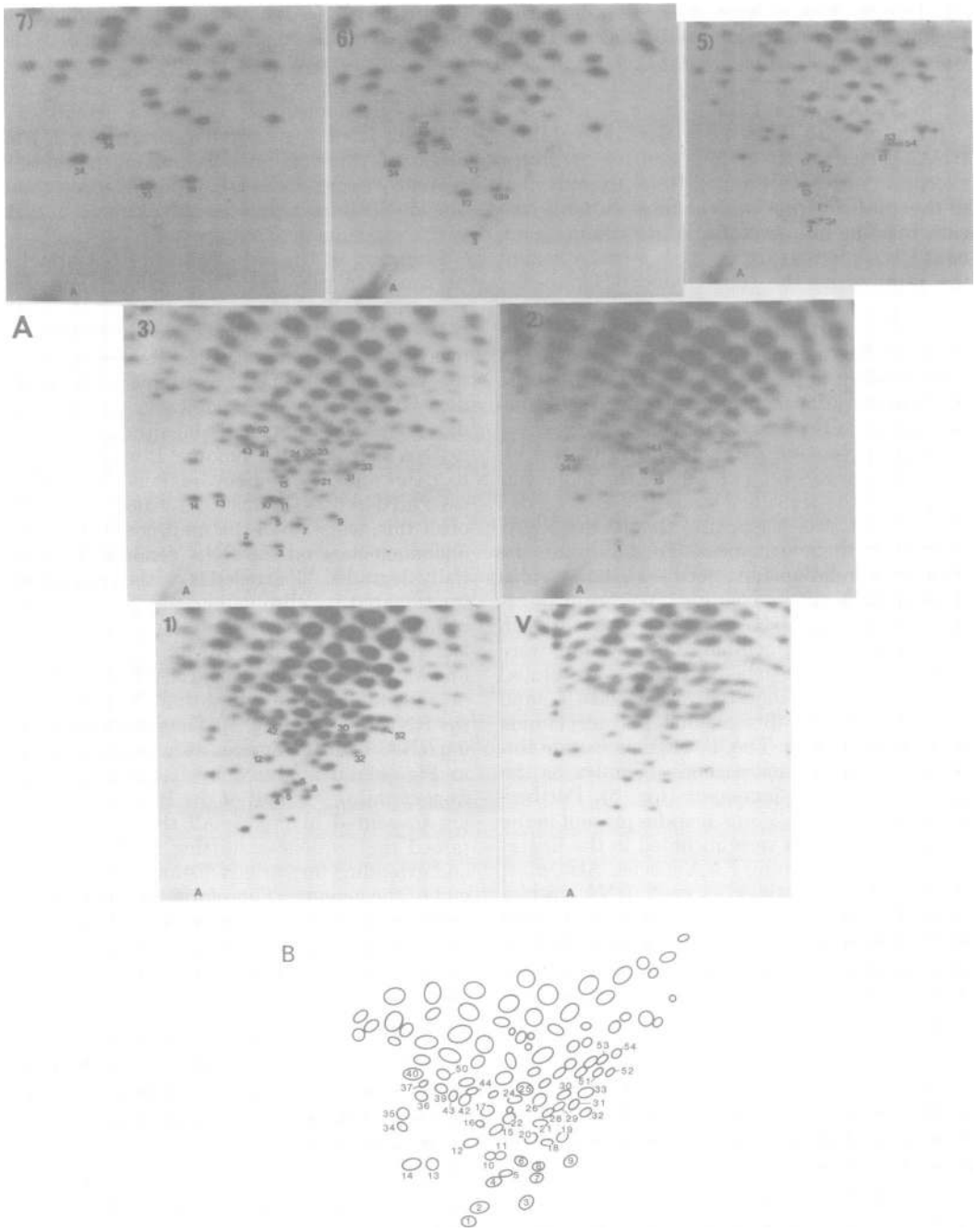

FIG. 3. *Oligonucleotide fingerprinting of the intracellular A59-specific RNAs. The virus-specific RNAs were eluted from agarose gels, digested with RNase T_1, and separated by two-dimensional polyacrylamide gel electrophoresis. Electrophoresis was from left to right in the first dimension and from bottom to top in the second dimension. The numbering of the spots is as indicated in the schematic sketch (B). Only the oligonucleotides which appeared for the first time in the mRNA's of increasing size were numbered. The numbers at the upper left corners of each panel represent the RNA species referred to in Fig. 2. Abbreviations: V, virion genomic RNA; A, poly(A).*

from the viral genome or were not contiguous with the rest of the oligonucleotides on the genome. Whether these oligonucleotides represent splicing of the sequences is unknown at the

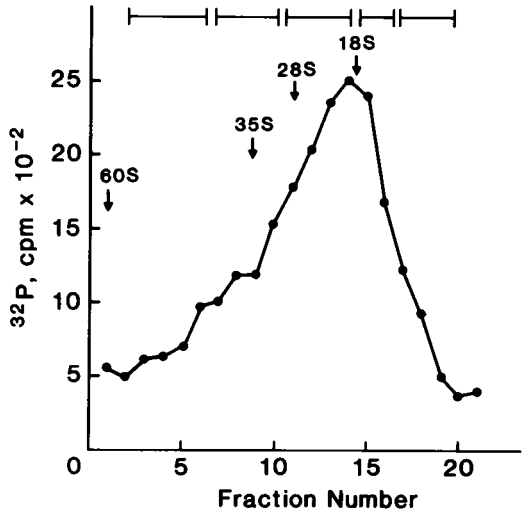

FIG. 4. *Sucrose gradient sedimentation of the partially degraded poly(A)-containing A59 genomic RNA. The poly(A)-containing fraction from the partially degraded A59 RNA was selected by oligo(dT)-cellulose column chromatography and sedimented on a 10 to 25% sucrose gradient made in 0.01 M Tris hydrochloride, pH 7.4, 0.01 M NaCl, and 0.05% SDS in an SW41 rotor at 40,000 rpm for 4.5 h. The RNA of different sizes was pooled into the five fractions as indicated.*

present time.

Sequences immediately adjacent to the 3' ends of the virus-specific RNAs. The oligonucleotide mapping studies suggested that all of the virus-specific RNAs contained the oligonucleotides starting from the 3' end of the genome. Thus, they should have identical 3' end sequences. However, this conclusion was uncertain since several RNA species contained oligonucleotides not present in the genome, and some of the oligonucleotides in the smaller RNA species were not present in the larger RNAs. It was therefore possible that some of these RNAs might have different 3'-end sequences. To test this possibility, the poly(A) spots from the oligonucleotide fingerprints of each RNA (Fig. 3) were isolated, digested with RNase A, and separated by electrophoresis on DEAE-cellulose paper at pH 3.5. These poly(A) spots should contain not only the poly(A) tracks but also the sequences which are immediately adjacent to the poly(A) and extend inward until the first guanine residue. Figure 7 shows such an analysis for RNAs 5, 6, and 7. From the molar yields of each base, the base composition of the sequences immediately adjacent to the poly(A) spots was determined to contain $C(AC)(AG)(A_2U)(A_3C)(A_4N)A_{101-130}$ (Table 2). It can be seen that all of the RNAs contained identical base compositions and likely had identical sequences at the 3' end. These data also show that all of the RNA species contained a poly(A) stretch of 100 to 130 nucleotides long. The presence of (AG) residues within this stretch cannot be explained at the present time. It was reproducible and may represent sequences protected from RNase T_1 digestion by the poly(A) stretch. Similar studies have been performed with the poly(A) spots of the RNAs 1, 2, and 3. All of them appeared to have the same base sequences, although the molar yield of each base was not confirmed by counting radioactivity because of the low counts associated with each spot (data not shown). These data therefore suggest that all the virus-specific RNA species contained identical 3' end sequences.

Genetic localization of the sequence divergence between A59 and MHV-3. We have previously shown that A59, a weakly pathogenic strain, and MHV-3, a strongly hepatotropic strain, have very similar oligonucleotide fingerprints except for two unique oligonucleotides in MHV-3 and four in A59 (7). Some of these oligonucleotides might be derived from the genetic regions responsible for the biological differences between these two virus strains. We therefore attempted to localize these oligonucleotides on the RNA genome. As shown previously, A59 contains four unique oligonucleotides, 9, 13, 19, and 28, which are not present in MHV-3 (7). Comparison of Fig. 3 with Fig. 5 shows that two of the A59-specific oligonucleotides, 9 and 13, were present in the genetic region at 6 to 10 kilobases from the 3' end which corresponds to RNA 3 (Fig. 6). In contrast, the genetic localization of the oligonucleotides 19 and 28 is less certain. Although oligonucleotide 19 appeared to be present in RNA 7, it was absent in RNAs 5 and 6. Oligonucleotide 28 appeared also to be present in RNA 3 (Fig. 3), but it was found by fingerprinting degraded virion RNA to be closer to the 5' end of the genome (Fig. 5). This oligonucleotide was present at lower molar yields than other oligonucleotides, thus increasing the difficulty of precise genetic mapping. The oligonucleotide 28 was therefore not represented in Fig. 6.

We also mapped the two MHV-3-specific oligonucleotides, *a* and *b*, on the RNA genome by fingerprinting the poly(A)-containing RNA of different size fractions. Figure 8 shows some of the representative fingerprints. By this approach, it was determined that *a* was localized at 6 to 7 kilobases from the 3' end, whereas *b* was localized very close to the 5' end. These two regions correspond to the regions contained within RNA 3 and RNA 1, respectively. From

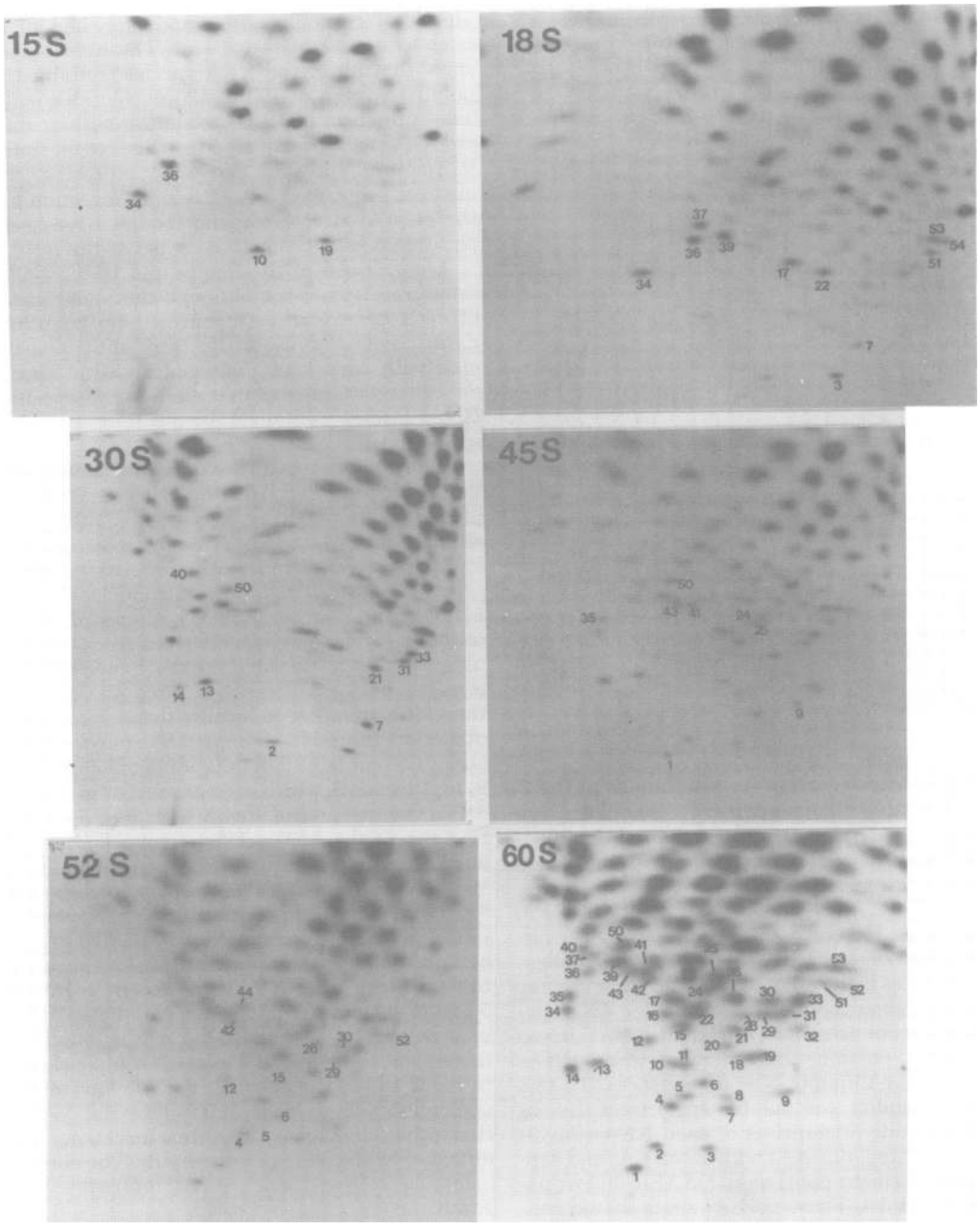

FIG. 5. *T_1-oligonucleotide fingerprints of the poly(A)-containing A59 RNAs of different size fractions. The RNAs collected as indicated in Fig. 4 were analyzed by T_1 oligonucleotide fingerprinting. Oligonucleotides which appeared for the first time in the RNAs of increasing size were numbered. The numbering of the total large T_1 oligonucleotides is shown for the 60S RNA and is identical to that in Fig. 3(B).*

the genetic maps of A59 and MHV-3, we concluded that at least RNAs 3 and 1 contained the genetic differences between these two strains.

DISCUSSION

Our results show that L-2 cells infected with the A59 strain of MHV contain six to seven

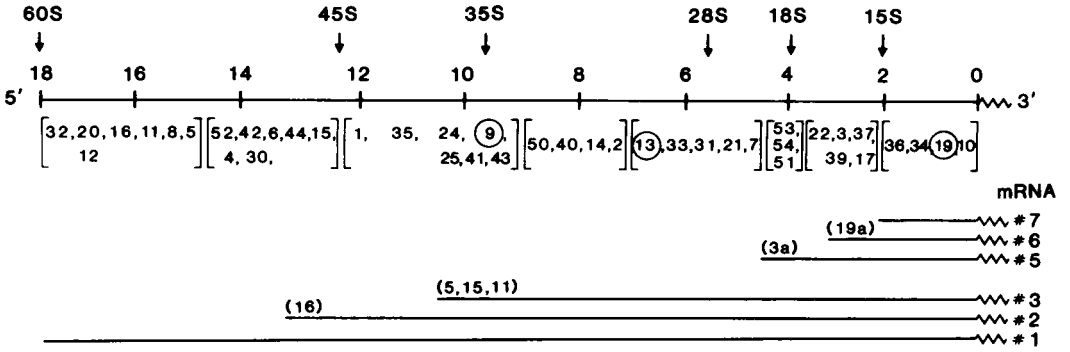

FIG. 6. *Oligonucleotide map of the A59 genome and its corresponding subgenomic RNAs. The T_1 oligonucleotides of the A59 genomic RNA (numbered as shown in Fig. 3 and 5) were arranged into several groups on different regions of the genome. Since the genomic RNA has a molecular weight of 5.4×10^6, the genome length is assumed to be 18 kilobases. The subgenomic RNAs are also presented. The oligonucleotides in parentheses on different subgenomic RNAs either were absent from the genomic RNA or were not localized in the corresponding regions of the genome. Oligonucleotides in common with those on the genomic RNA were not labeled on the subgenomic RNAs. The circled spots, 9, 13, and 19, are specific for A59 and not present in MHV-3 (7).*

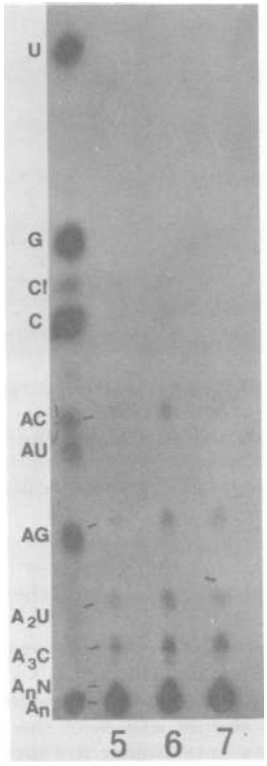

FIG. 7. *Base sequence analysis of the poly(A)-containing oligonucleotides of the A59 mRNA's. The poly(A)-containing oligonucleotides were isolated from the oligonucleotide fingerprints of each virus-specific RNA species as shown in Fig. 3. These oligonucleotides were digested with RNase A and electrophoresed on DEAE-cellulose paper in acetic acid-pyridine buffer, pH 3.5, at 1,500 V for 4 h. The 60S RNA digested with RNase A and T_1 was included as mono- and oligonucleotide markers (3). The relative ratio of each spot was determined. Only those from the mRNA's 7, 6, and 5 are shown here. Abbreviations: A, AMP; C, CMP; G, GMP; U, UMP; C!, cyclic CMP; N, any nucleotides other than AMP.*

TABLE 2. *Partial base sequence analysis of the 3'-end sequences*[a]

RNA species	Base composition
5	$C(AC)(AG)(A_2U)(A_3C)(A_4N)A_{101}$
6	$C(AC)(AG)(A_2U)(A_3C)(A_4N)A_{113}$
7	$C(AC)(AG)(A_2U)(A_3C)(A_4N)A_{130}$

[a] The poly(A)-containing oligonucleotides were eluted from the two-dimensional fingerprints, digested with RNase A, and separated by electrophoresis on DEAE-cellulose paper at pH 3.5 (Fig. 1). Each spot was cut out, and the relative ratio of each spot was determined by counting in toluene-based scintillation fluid.

virus-specific RNA species. Similar findings have recently been obtained with other cell lines, including Sac (−) and 17 Cl-1 cells (13; Wege et al., in press; J. L. Liebowitz, K. C. Wilhelmsen, and C. W. Bond, personal communication). However, in L-2 cells, one of the al., in press; Liebowitz et al., personal communication). However, in L-2 cells, one of the RNAs, 4, was not always detectable or present only in very low quantity. It is not clear whether this variance represents a host cell-determined differential expression of viral RNA. We have also shown that all of the virus-specific RNAs contain poly(A) segments of 100 to 130 nucleotides long. This is similar to the length of the poly(A) present in the viral genome, which has been estimated to be about 90 nucleotides long (21).

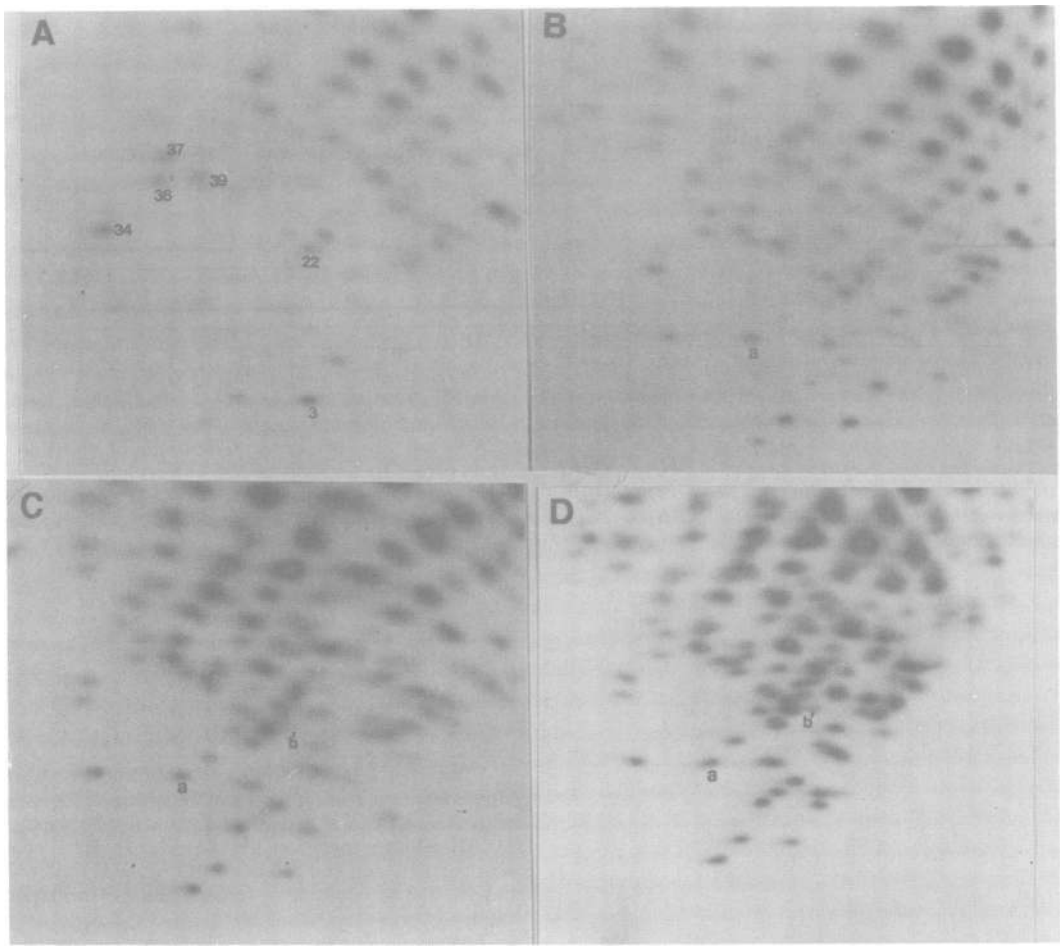

FIG. 8. *Oligonucleotide fingerprints of the partially degraded, poly(A)-containing MHV-3 genomic RNA species. The ^{32}P-labeled, 60S MHV-3 RNA was briefly digested, selected by oligo(dT)-cellulose chromatography, and sedimented by sucrose gradient sedimentation as described for MHV-A59 (Fig. 4). The representative RNA fractions were pooled and analyzed by T_1 oligonucleotide fingerprinting. Only representative fingerprints are shown here. (A) 18S; (B) 35S; (C) 50S; (C) 60S. Oligonucleotides a and b are specific for MHV-3 and not present in A59 (7).*

The presence of poly(A) sequences in these RNAs suggests that they represent mRNA's. This conclusion is consistent with the recent findings that these virus-specific RNAs were present in the polysome fractions of MHV-infected cells (M. M. C. Lai, C. D. Patton, and S. A. Stohlman, unpublished data; 13) and that these RNAs could serve as mRNA's for in vitro translation (12; S. Siddell, H. Wege, A. Barthel, and V. ter Meulen, *in* V. ter Meulen, S. Siddell, and H. Wege, ed., *Biochemistry and Biology of Coronaviruses*, in press).

The structure of these viral mRNA's contains some very unusual features. The oligonucleotide fingerprinting studies suggest that they have a "nested structure," as termed by Stern and Kennedy (14, 15); i.e., the sequences of the small mRNA are contained within the next-larger mRNA species. Furthermore, the mapping of the oligonucleotides on the genome suggests that the sequences of all of these mRNA's start from the 3′ end of the genome. These data strongly suggest that the structures of the mRNA's of MHV-A59 are very similar to that of avian infectious bronchitis virus (14, 15). In further support of this proposal, we found that all of the mRNA species contained identical sequences immediately adjacent to the 3′-poly(A). The presence of several anomalous oligonucleotides in some mRNA species, however, suggests that MHV mRNA's might be more complex than the infectious bronchitis virus model. Some oligo-

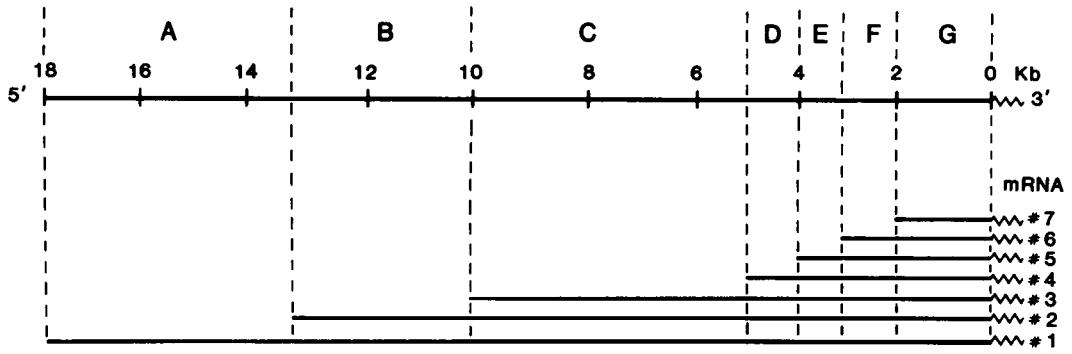

FIG. 9. *Proposed model of the structure of the MHV mRNA's and the corresponding genetic regions on the genome. The proposed seven genetic regions on the MHV genome are based on the data reported here and from other laboratories (13; Wege et al., in press; Leibowitz, personal communication). The boundaries of each gene were estimated by converting the molecular weights of the RNAs into kilobases (kb). Each gene corresponds to the portion of each mRNA species which does not overlap with the next-smaller mRNA species.*

nucleotides were present in the smaller mRNA's but not in the larger RNAs, whereas others were not present in the genome. These findings suggest that the 5' ends of these mRNA's could be quite unusual. Preliminary data suggest that all of them contain the cap sequences at the 5' ends. We are currently investigating the oligonucleotides which might contain such a cap structure.

The mRNA's with such a stairlike relationship are very similar to those found in retroviruses and togaviruses (5, 16, 21). In these mRNA's, usually only the portion of the sequences which is unique to a particular mRNA species and which is not shared with the next-smaller mRNA is translated. If a similar relationship of mRNA's to genome occurs during replication of MHV, the MHV RNA genome could be divided into seven genetic regions corresponding to these mRNA species (Fig. 9). This model offers a rational basis for studying the genetic structure of the RNA genome of MHV. The coding potentials of the mRNA's in another strain of MHV, JHM, have been studied by in vitro translation (12; Siddell et al., in press). If these data can be applied to the A59 strain, it could suggest that the gene products of the following genes are: for *B*, a nonstructural protein p30; for *C*, gp180/90; for *D* or *E*, nonstructural p14; for *F*, gp23; and for *G*, pp60. In analogy to other virus systems, gene *A* might code for an RNA polymerase. It remains to be investigated whether MHV-A59 codes for similar products.

The study of the oligonucleotide maps of all of the mRNA species has also allowed us to localize the genetic differences between two MHV strains, MHV-3 and A59. Previously, we have shown that these two strains differ only slightly in their oligonucleotide fingerprints (7). Since these two strains are genetically related but differ in their pathogenic potentials—MHV-3 causes severe hepatitis, whereas A59 is only weakly pathogenic—these oligonucleotide differences could suggest the genetic regions responsible for such pathogenic potentials (7). Our mapping studies indicate that one of these regions might correspond to mRNA 3 and thus would reside in gene *C*, which codes for gp90/180, whereas the other corresponds to mRNA 1 and therefore would reside in gene *A*, which might code for an RNA polymerase. Whether these two regions are directly responsible for the viral pathogenicity remains to be investigated. If gene *C* is indeed responsible for the viral pathogenicity, it will suggest an interesting mechanism for viral pathogenesis: the gene product of this gene, gp 90/180, is the major envelope glycoprotein in MHV (17) and could determine the host range of the virus. The nonpathogenic strain, A59, might have mutations in this gene and thus became unable to infect the target cells. Further studies are required to resolve this issue.

ACKNOWLEDGMENTS

We thank T. Hanson for excellent technical assistance and J. Lopez for editorial help.

This work was supported in part by grant PCM-4567, awarded by the National Science Foundation, and by Public Health Service grants NS 15079 and CA 16113, awarded by the National Institutes of Health.

ADDENDUM IN PROOF

We have recently shown that all of the A59-specific RNAs contain identical 5' end sequences, suggesting synthesis of these RNAs by splicing or another unusual mechanism (M. M. C. Lai, C. D. Patton, and S. A. Stohlman, submitted for publication).

LITERATURE CITED

1. **Aviv, H., and P. Leder.** 1972. Purification of biologically active globin messenger RNA by chromatography in oligothymidylic acid-cellulose. Proc. Natl. Acad. Sci.

U.S.A. **59**:1408–1412.
2. **Bailey, J. M., and N. Davidson.** 1976. Methylmercury as a reversible agent for agarose gel electrophoresis. Anal. Biochem. **70**:75–85.
3. **Barrell, B. G.** 1971. Fractionation and sequence analysis of radioactive nucleotides, p. 751–779. *In* G. L. Cantoni and D. R. Davies (ed.), Procedures in nucleic acid research, vol. 2. Harper & Row, Publishers, New York.
4. **Guy, J. S., and D. A. Brian.** 1979. Bovine coronavirus genome. J. Virol. **29**:293–300.
5. **Hayward, W. S.** 1977. Size and genetic content of viral RNAs in avian oncovirus-infected cells. J. Virol. **24**:47–63.
6. **Lai, M. M. C., and S. A. Stohlman.** 1978. RNA of mouse hepatitis virus. J. Virol. **26**:236–242.
7. **Lai, M. M. C., and S. A. Stohlman.** 1981. Comparative analysis of RNA genomes of mouse hepatitis viruses. J. Virol. **38**:661–670.
8. **Lomniczi, B., and I. Kennedy.** 1977. Genome of infectious bronchitis virus. J. Virol. **24**:99–107.
9. **MacNaughton, M. R., and M. H. Madge.** 1978. The genome of human coronavirus strain 229E. J. Gen. Virol. **39**:497–504.
10. **McIntosh, K.** 1973. Coronaviruses: a comparative review. Curr. Top. Microbiol. Immunol. **63**:85–129.
11. **Robb, J. A., and C. W. Bond.** 1979. Pathogenic murine coronaviruses. I. Characterization of biological behavior in vitro and virus-specific intracellular RNA of strongly neurotropic JHM and weakly neurotropic A59V viruses. Virology **94**:352–370.
12. **Siddell, S. G., H. Wege, A. Barthel, and V. ter Meulen.** 1980. Coronavirus JHM: cell-free synthesis of structural protein p60. J. Virol. **33**:10–17.
13. **Spaan, W. J. M., P. J. M. Rottier, M. C. Horzinek, and B. A. M. van der Zeijst.** 1981. Isolation and identification of virus-specific mRNAs in cells infected with mouse hepatitis virus (MHV-A59). Virology **108**:424–434.
14. **Stern, D. F., and S. I. T. Kennedy.** 1980. Coronavirus multiplication strategy. I. Identification and characterization of virus-specific RNA. J. Virol. **34**:665–674.
15. **Stern, D. F., and S. I. T. Kennedy.** 1980. Coronavirus multiplication strategy. II. Mapping the avian infectious bronchitis virus intracellular RNA species to the genome. J. Virol. **36**:440–449.
16. **Strauss, J. H., and E. G. Strauss.** 1977. Togaviruses, p. 111–166. *In* D. P. Nayak (ed.), The molecular biology of animal viruses. Marcel Dekker, Inc., New York.
17. **Sturman, L. S.** 1977. Characterization of a coronavirus. I. Structural proteins: effects of preparative conditions on the migration of protein in polyacrylamide gels. Virology **77**:637–649.
18. **Tyrrell, D., J. Almeida, C. Cunningham, W. Dowdle, M. Hofstad, K. McIntosh, M. Tajima, R. Zakstelskaya, B. Esterday, A. Kapikian, and R. Bingham.** 1975. Coronaviridae. Intervirology **5**:76–82.
19. **Wege, H., A. Muller, and V. ter Meulen.** 1978. Genomic RNA of the murine coronavirus JHM. J. Gen. Virol. **41**:217–227.
20. **Weiss, S. R., H. E. Varmus, and J. M. Bishop.** 1977. The size and genetic composition of virus-specific RNAs in the cytoplasm of cells producing avian sarcoma-leukosis viruses. Cell **12**:983–992.
21. **Yogo, Y., N. Hirano, S. Hino, H. Shibuta, and M. Matumoto.** 1977. Polyadenylate in the virion RNA of mouse hepatitis virus. J. Biochem. **82**:1103–1108.